lncRNA1471 mediates tomato-ripening initiation by binding to the ASR transcription factor

Lingling Zhang[1,2], Guoning Zhu[1], Liqun Ma[1], Tao Lin[3], Andrey R. Suprun[4], Guiqin Qu[1], Daqi Fu[1], Benzhong Zhu[1], Yunbo Luo[1] and Hongliang Zhu[1,*] (iD)

[1]*College of Food Science and Nutritional Engineering, China Agricultural University, Beijing 100083, China,*

[2]*School of Public Health, Key Laboratory of Environmental Factors and Chronic Disease Control, Ningxia Medical University, Yinchuan, Ningxia, Hui Autonomous Region 750004, China,*

[3]*College of Horticulture, China Agricultural University, Beijing 100193, China, and*

[4]*Federal Scientific Center of the East Asia Terrestrial Biodiversity, Far Eastern Branch of the Russian Academy of Sciences, Vladivostok, Russia*

SUMMARY

The regulatory mechanisms underlying fruit ripening, including hormone regulation, transcription factor activity, and epigenetic modifications, have been discussed extensively. Nonetheless, the role of long non-coding RNAs (lncRNAs) in fruit ripening remains unclear. Here, we identified *lncRNA1471* as a negative regulator of tomato fruit-ripening initiation. Knocking out *lncRNA1471* via large fragment deletion resulted in accelerated initiation of fruit ripening, a shorter color-breaking stage (BR), deeper coloration, increased levels of ethylene, lycopene, and β-carotene, accelerated chlorophyll degradation, and reduced fruit firmness. These phenotypic changes were accompanied by alterations in the carotenoid pathway flux, ethylene biosynthesis, and cell wall metabolism, primarily mediated by the direct regulation of key genes involved in these processes. For example, in the *CR-lncRNA1471* mutant, lycopene-related *SlPSY1* and *SlZISO* were upregulated. Additionally, the expression levels of ethylene biosynthetic genes (*SlACS2* and *SlACS4*), ripening-related genes (*RIN*, *NOR*, *CNR*, and *SlDML2*), and cell wall metabolism genes (*SlPL*, *SlPG2a*, *SlEXP1*, *SlPMEI*-like, and *SlBG4*) were significantly upregulated, which further strengthening the findings mentioned above. Furthermore, *lncRNA1471* was identified to interact with the abscisic stress-ripening protein (ASR) transcription factor by chromatin isolation by RNA purification coupled with mass spectrometry (ChIRP-MS) and protein pull-down assay in *vitro*, which might regulate key genes involved in tomato ripening. The discovery of the significant non-coding regulator *lncRNA1471* enhances our understanding of the complex regulatory landscape governing fruit ripening. These findings provide valuable insights into the mechanisms underlying ripening, particularly regarding the involvement of lncRNAs in ripening.

Keywords: Tomato (*Solanum lycopersicum* L.), Fruit ripening, lncRNA, Gene editing, ChIRP-MS.

INTRODUCTION

Long non-coding RNAs (lncRNAs) are characterized by nucleotide length (>200-nt) originating via distinct mechanisms and involving epigenetic, transcriptional control, and post-transcriptional modification (Wierzbicki et al., 2021). Specifically, lncRNAs serve as sources of endogenous small interfering RNAs (endo-siRNAs) through dicer-mediated cleavage or as interacting factors with viral siRNAs (Borsani et al., 2005; Yang et al., 2019). Furthermore, lncRNAs often act as molecular sponges for miRNAs to modulate the expression of their target mRNAs (Thomson & Dinger, 2016). A distant lncRNA, *APOLO*, originates from a genomic locus located approximately 5 kb upstream of PID. A chromosomal loop forms between lncRNA *APOLO* and the *PID* promoter that mainly recruits epigenetic marks such as histone H3 lysine 27 trimethylation (H3K27me3) and DNA methylation, regulating auxin transport in *Arabidopsis* (Ariel et al., 2014). Certainly, lncRNAs interact with various proteins to modulate protein activity, serve as protein structural complexes, and alternate protein localization within

cellular compartments (Wilusz et al., 2009). Recently, chromatin isolation by RNA purification coupled with mass spectrometry (ChIRP-MS) has emerged as a highly effective and precise strategy for identifying lncRNA-interacting proteins *in vivo* (Pierouli et al., 2021). For instance, researchers detected that lncRNA *MISSEN* bound to the helicase family protein (HeFP) and regulated rice endosperm development using the ChIRP-MS method (Zhou et al., 2021).

Fruit ripening is a critical stage for seed dispersal and fruit quality (Alba et al., 2005). The regulation of tomato ripening involves hormonal influences, transcription factors, and epigenetic modifications (Qin et al., 2012; Zhong et al., 2013). As the tomato ripens, the two most notable phenotypic characteristics are alterations in fruit color and firmness (Deng et al., 2022; Fraser et al., 1994). The most well-known hormone, ethylene, directly influences tomato fruit ripening (Nakatsuka et al., 1998). Furthermore, depending on ethylene, gibberellin partially mediates auxin and abscisic acid signaling during tomato ripening and softening (Wu et al., 2024). Regarding transcription factors, various ripening-impaired nature mutants have been identified, including *Rin* (*ripening-inhibitor*), *Nor* (-*non-ripening*), *Cnr* (*colorless non-ripening*), and *Nr* (*never-ripe*, an ethylene receptor) (Barry et al., 2005; Giovannoni, 2004; Manning et al., 2006; Vrebalov et al., 2002). Additionally, epigenetic modifications mainly involve DNA methylation, RNA editing, and histone modifications (Hu et al., 2021). For example, cytidine-to-uridine RNA-editing factor *slorrm4* mutants delayed tomato fruit ripening (Yang et al., 2017).

Recently, The genome-wide identification and characterization of lncRNAs in various plants have been reported, such as *Cucumis melo* (Tian et al., 2019), *Cucumis sativus L.* (Dey et al., 2022), watermelon (Yu et al., 2023), *Vaccinium corymbosum L.* (Li et al., 2022), and others. Moreover, our team and other groups have explored regulatory mechanisms of fruit ripening from the perspective of lncRNAs. Our pioneering study identified 3679 long intergenic non-coding RNAs (lincRNAs) in *rin* mutants, emerging 490 upregulated lncRNAs and 187 downregulated lncRNAs (Zhu et al., 2015). We subsequently found that *lncRNA1459* and *lncRNA1840* might influence lycopene accumulation and ethylene production, delaying tomato fruit ripening (Li et al., 2018; Zhu et al., 2024). Furthermore, our team elucidated that *lncRNA2155* is a *rin*-directed binding target to postpone tomato fruit ripening (Yu et al., 2019). In the *nr* mutant, researchers identified some targets of lncRNAs exhibiting 5-methylcytosine (m5C) sites, suggesting a potential involvement in methylation activity that affects fruit ripening (Guo et al., 2022). Thirty-one differentially expressed lncRNAs co-located with genes were

associated with kiwifruit ripening (Chen et al., 2021). Moreover, lncRNA *FRILAIR* possesses a highly conserved binding site for *miR397*, and its overexpression significantly enhances strawberry ripening (Tang et al., 2021).

Although numerous lncRNAs associated with fruit ripening have emerged through genome-wide studies, direct validation of specific lncRNAs implicated in fruit ripening remains limited. Building on previous research, we identified that *lncRNA1471* regulates tomato ripening. Using our advanced CRISPR-Cas9-editing technology (Zhu et al., 2023), we generated an *lncRNA1471* knockout mutant with a large fragment deletion. The *CR-lncRNA1471* mutant accelerated the initiation of fruit ripening compared to the WT and triggered a range of phenotypic and genetic alterations, resulting in shorter BR time, deeper coloration, increased levels of ethylene, lycopene, and β-carotene, accelerated chlorophyll degradation, and reduced fruit firmness. Additionally, significant alterations were observed in the expression patterns of ripening-related genes in the *lncRNA1471* knockout mutant. Furthermore, *lncRNA1471* was identified to interact with the abscisic stress-ripening protein ASR transcription factor *in vivo* and *in vitro*, which may regulate the key genes involved in tomato ripening. Taken together, the discovery of *lncRNA1471* enhances our understanding of the complex regulatory landscape governing fruit ripening. It offers significant insights into the mechanisms of ripening from the perspective of lncRNA involvement.

RESULT

LncRNA1471 expressed specifically in tomato fruit

Our previous research has elucidated some lncRNAs associated with tomato ripening (Zhu et al., 2015). We identified *lncRNA1471*, located on chromosome 3 (SL2.50ch03), characterized by a poly (A)$^+$ tail and a 5′ 7-methyl guanylate cap. The transcript was devoid of introns and had a full-length sequence of 850 bp, including a 21 bp length of the 3′UTR region and a 157 bp length of the 5′UTR region (Figure 1A). Full-length sequence data were illustrated in Figure S1 and were submitted to the GenBank database (No. 2664405). Additionally, *lncRNA1471* also significantly characterized non-coding features using the online website (CPC2, https://cpc2.gao-lab.org/index.php), with protein-coding genes (*ACS2* and *MADS-RIN*) and lncRNAs (*APOLO* and *COOLAIR*) as controls (Figure 1B). Analysis of the expression patterns of *lncRNA1471* in tomatoes revealed peak expression in the fruit organism (Figure 1C). We also separated the nuclear and cytoplasmic fractions from tomato fruit at 45 days post-anthesis (DPA), and *lncRNA1471* was detected in both the cytoplasm

and nucleus, with a slightly higher abundance observed in the cytoplasmic fraction (Figure 1D). These results suggest that *lncRNA1471* is predominantly expressed in the cytoplasm and nucleus of tomato fruits. These findings indicated that *lncRN1471* may play a role in tomato ripening through diverse regulatory mechanisms.

© 2025 Society for Experimental Biology and John Wiley & Sons Ltd.,
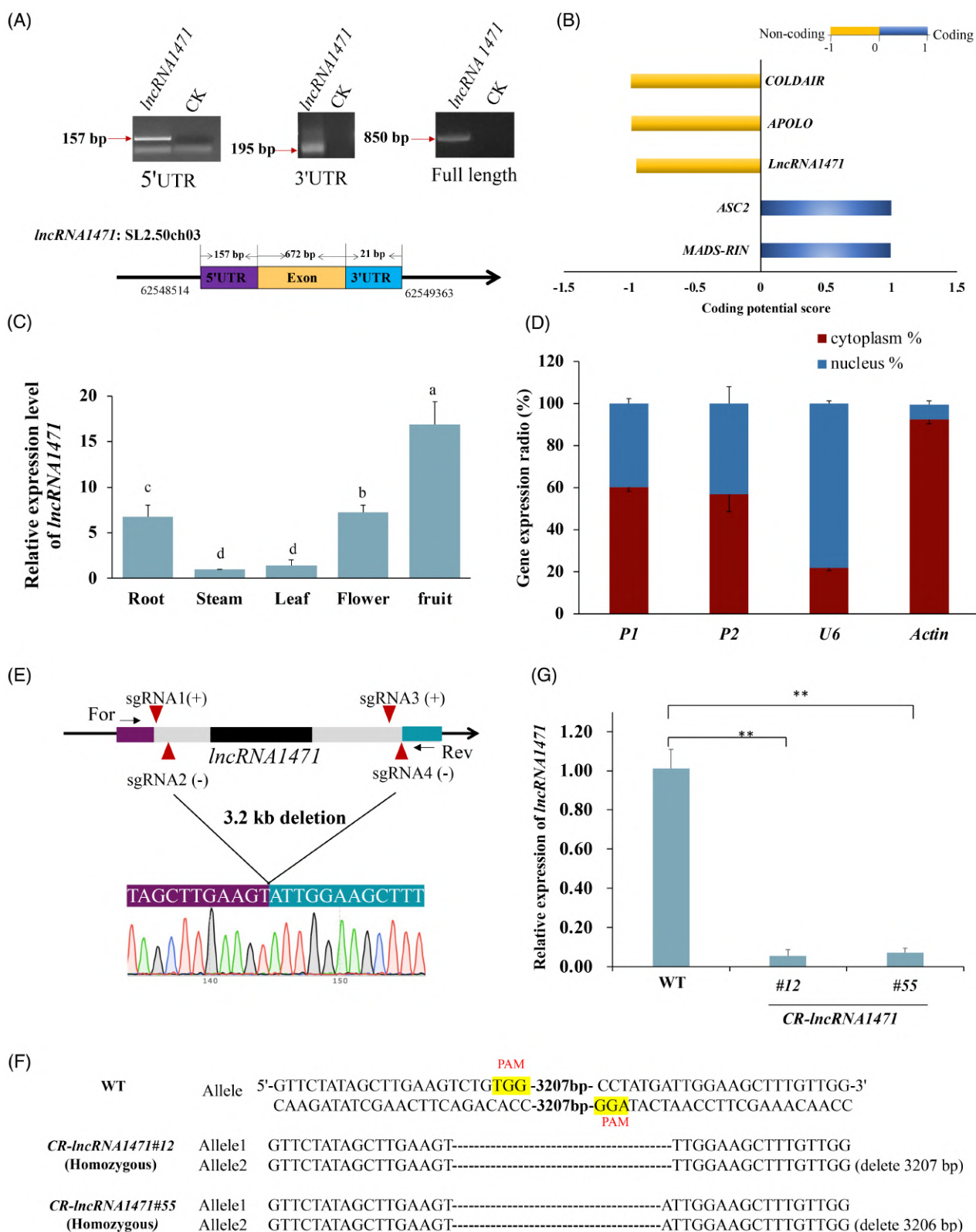
Figure 1. Molecular characteristics of *lncRNA1471*.
(A) Full-length cloning of *lncRNA1471* using H_2O as a control (CK).
(B) Predictive non-coding information for *lncRNA1471*.
(C) Expression patterns of *lncRNA1471* in tomato tissues.
(D) Subcellular localization of *lncRNA1471*, with the *U6* and *Actin* genes selected as internal controls for nuclear and cytoplasmic fragments, respectively. Both P1 and P2 were primers for *lncRNA1471*.
(E) Schematic diagram of the sgRNA site in the neighboring area of *lncRNA1471*. Red triangles indicate the four sgRNA sites. The black frame represents *lncRNA1471*, and the gray area denotes the upstream or downstream region of *lncRNA1471*. Purple and dark green represent sequences of upstream or downstream regions of sgRNA1 and sgRNA4, respectively. The arrow represents RT-qPCR primers for *lncRNA1471*.
(F) The genotype of WT, *CR-lncRNA1471#12*, and *CR-lncRNA1471#55* homozygous mutants in the T1 generation. Yellow lettering represents the PAM sequence.
(G) *LncRNA1471* expression level in representative lines of the T1 generation. The relative level of *lncRNA1471* expression in the WT was assigned as the reference standard and was normalized to the *actin* expression level.

Knockout of *lncRNA1471* promotes the initiation of tomato fruit ripening

To investigate potential biological functions, we generated knockout mutants of *lncRNA1471* using the double-reverse pairs of sgRNAs strategy within the CRISPR-Cas9 system to disrupt the secondary structure of *lncRNA1471* (Zhu et al., 2023). Following the design principles (Zhu et al., 2023), we built a pair of sgRNAs strategically positioned in the upstream and downstream regions of *lncRNA1471*, respectively (Figure 1E). A pair of primers (For and Rev) was designed to amplify a 483 bp residual fragment sequence following the deletion of a large fragment, including *lncRNA1471* (Figure S2). Therefore, we successfully deleted a substantial fragment between sgRNA1 and sgRNA4 from the first generation (T0). As anticipated, we identified two distinct deletion types in the secondary generation transgenic plants (T1): *CR-lncRNA1471#12* deleted 3207 bp and *CR-lncRNA1471#55* deleted the 3206 bp fragment (Figure 1F). Therefore, *lncRNA1471* was barely expressed in either knockout mutant (Figure 1G). Simultaneously, we generated overexpression mutants of *lncRNA1471* using the cauliflower mosaic virus (CaMV) 35S promoter, resulting in 19 independent OE-*lncRNA1471* mutants in the T0 generation. The top two lines with the highest expression levels, OE-*lncRNA1471#2* and OE-*lncRNA1471#8*, were selected for subsequent experiments (Figure S3).

Furthermore, *CR-lncRNA1471* (#12, #55) exhibited a shorter BR period than WT in the T1 generation. In contrast, *OE-lncRNA1471* (#2, #8) displayed a BR period similar to WT (Figure 2A). Because of the phenotypic similarities observed among various plant lines with the same genotype, we selected CR-*lncRNA1471#12* and OE-*lncRNA1471#2* as representative plants for subsequent research. Certainly, the *CR-lncRNA1471#12* mutant reached the BR stage at 40 DPA, which was significantly earlier than both WT fruits (44 DPA) and OE-*lncRNA1471#2* mutants (44 DPA) (Figure 2B). These findings illustrate that the knockout of *lncRNA1471* promotes the initiation of tomato ripening and results in earlier fruit ripening.

Knockout of *lncRNA1471* promoted ethylene emission, lycopene accumulation, and fruit firmness reduction

To elucidate the effect of *lncRNA1471* on tomato ripening, we compared the ripening states of *CR-lncRNA1471*, the *OE-lncRNA1471* mutant, and the WT. Tomato is universally recognized as a climatic fruit, characterized by ethylene bursts (Giovannoni, 2004). Accordingly, we measured ethylene production and found that the *CR-lncRNA1471#12* mutant reached its ethylene peak (43 DPA) earlier than the WT and *OE-lncRNA1471#2* (49 DPA). The ethylene peak consistently emerged on the 3rd day after the BR stages, with no discernible variation in peak ethylene levels in any plant line (Figure 2C). Before reaching 46 DPA, ethylene emission in the knockout mutants exceeded that in both the WT and OE mutants. Furthermore, the fruits at the BR stage were treated with 3.5% 1-MCP. In the 1-MCP treatment groups, the inhibition rate of ripening progression in the *CR-lncRNA1471* mutant, WT, and OE-

Figure 2. Observation of ripening-related phenotypic traits across various plant lines in the T1 generation.
(A) Phenotypes of independent homozygous mutants at different developmental stages in the T1 generation. The representative plant lines for each mutant line are *CR-lncRNA1471#12–5, CR-lncRNA1471#55–3, OE-lncRNA1471#2–4*, and *OE-lncRNA1471#8–1*.
(B) Statistical analysis of the DPA of independent homozygous mutants and WT.
(C) Determination of ethylene production.
(D) Determination of respiratory rate.
(E) Measurement of lycopene content.
(F) a* value of tomato fruit color.
(G) Determination of fruit firmness. Plant materials used for phenotypic observations across representative independent homozygous mutants including *CR-lncRNA1471#12, OE-lncRNA1471#2*, and WT. Error bars indicate ±SD based on triplicate biological replicates. In (B–G), blackish-green, orange, and turquoise colors represent the WT, *CR-lncRNA1471#12*, and O*E-lncRNA1471#2* mutants, respectively. DPA represents days post-anthesis. Samples marked with different lowercase letters indicate significant differences at $P < 0.05$, a single asterisk (*) represents $P < 0.05$, and the double asterisk (**) represents $P < 0.01$.
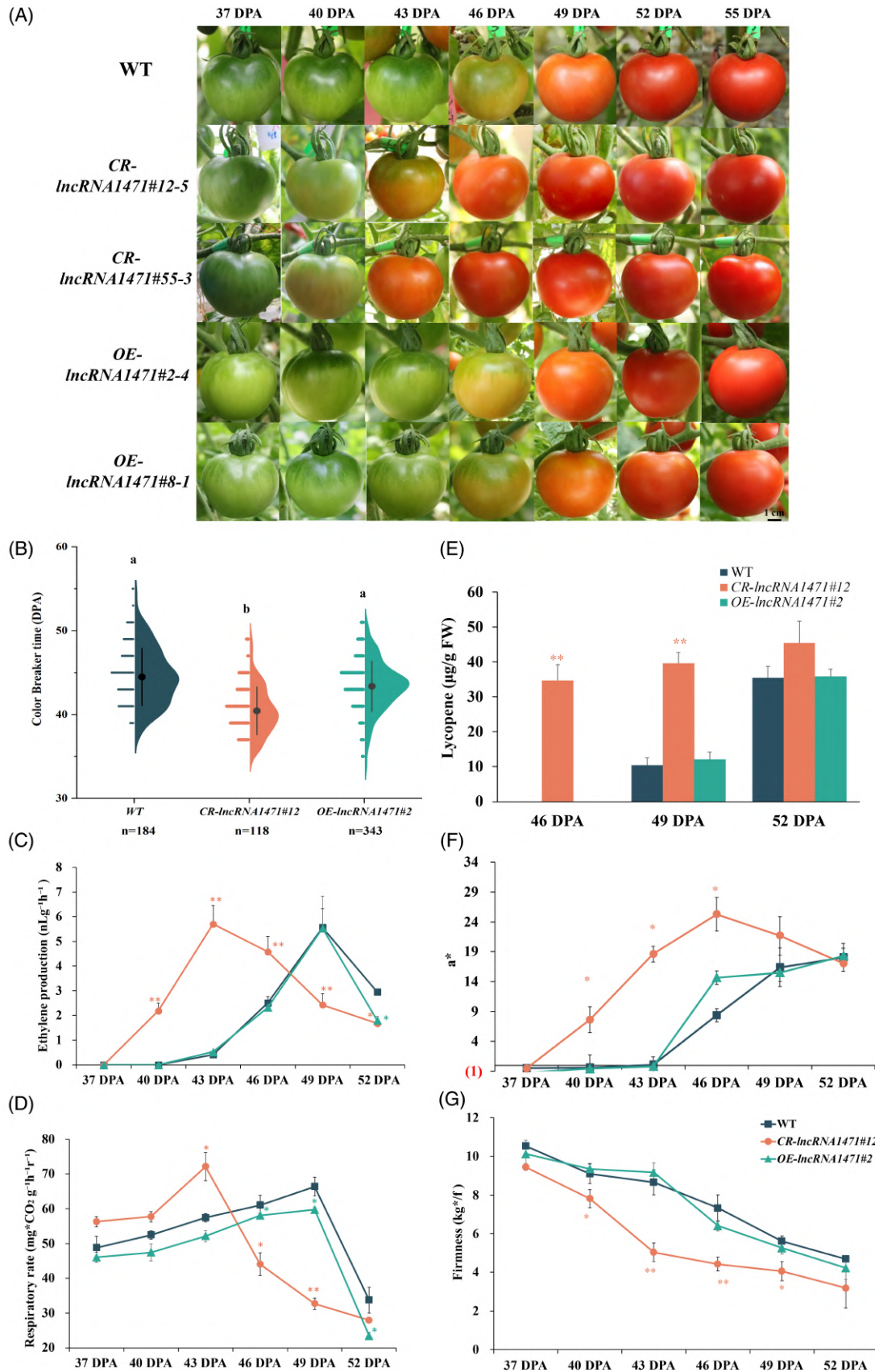
lncRNA1471#2 mutant was nearly identical, indicating that the ethylene signaling pathway functioned normally in the *CR-lncRNA1471* mutants (Figure S4). Additionally, the respiratory rate peak in *CR-lncRNA1471#12* mutants also occurred at 43 DPA, earlier than that in the WT and OE mutants (49 DPA) (Figure 2D). Therefore, *lncRNA1471* may be involved in the ethylene synthesis pathway rather than the ethylene signaling transmission pathway.

During tomato ripening, two of the most prominent features are fruit color turning and firmness reduction. *CR-lncRNA1471* mutants exhibited a noticeably deeper red hue than the WT and OE mutants at the same DPA (Figure 2A). Red coloration in tomato fruits is closely associated with lycopene accumulation and chlorophyll decomposition (Yang, Zhu, et al., 2020). At 46 and 49 DPA, the lycopene content of the knockout mutants was over 34 μg/g FW, whereas that of the WT and OE mutants was below 15 μg/g FW. However, no significant difference in lycopene content was observed among the plant lines at 52 DPA (Figure 2E). The metabolite of lycopene, β-carotene, continued to increase throughout the ripening process in the *CR-lncRNA1471* mutant and was consistently much higher than that in the WT and OE mutants (Figure S5). The a* color index value of *CR-lncRNA1471* mutants was significantly higher (Figure 2F). In addition, the total chlorophyll (Chl a + b) content was lower in the *CR-lncRNA1471* mutant than in the WT and *OE-lncRNA1471*#2 mutants (Figure S6).

The *CR-lncRNA1471#12* mutant exhibited a consistent decline in fruit firmness during the ripening period. Specifically, at 40 DPA, 43 PA, 46 DPA, and 49 DPA stages, fruit firmness was significantly reduced compared to the WT and *OE-lncRNA1471#2* mutants (Figure 2G). These results illustrate that knockout of *lncRNA1471* mainly affects ethylene biosynthesis, lycopene accumulation, chlorophyll degradation, and fruit firmness reduction, all of which reflect the phenotype of earlier fruit ripening. Therefore, *lncRNA1471* functions as a negative regulator of tomato-ripening initiation.

CR-lncRNA1471 mutant impaired the expression of ripening-related genes and lncRNAs

To investigate the underlying mechanisms responsible for the pronounced phenotypic changes in accelerated tomato-ripening initiation observed in the *CR-lncRNA1471* mutant, we performed transcriptome analysis of *CR-lncRNA1471* mutants and the WT at 40 DPA (Figure 3A). Due to the absence of distinct phenotypes in the OE lines, RNA-seq was not performed for these samples. All clean data were uploaded to the NCBI database (PRJNA1085275). Figure S7 demonstrated that the samples within each group owned strong reproducibility by principal component analysis (PCA) fitting. Based on the screening criteria (*P*-adj <0.05, |log$_2$FoldChange|>1) and alignment

to the tomato genome, 3331 significantly differentially expressed coding genes (DEGs) were identified, including 1215 upregulated DEGs and 2116 downregulated DEGs (Figure 3B; Table S1). A total of 486 differentially expressed lncRNAs were detected, containing 208 upregulated DELs and 278 downregulated DELs (Figure 3C, Tables S3, S4). Moreover, gene ontology (GO) analysis revealed that the upregulated DEGs were significantly involved in catalytic activity and transcription regulatory region nucleic acid binding. In contrast, the downregulated DEGs were primarily enriched in functions related to kinase activity, chlorophyll binding, cell walls, and biological regulation (Figure 3D). Moreover, Kyoto Encyclopedia of Genes and Genomes (KEGG) annotations indicated that the upregulated DEGs were predominantly involved in secondary metabolites, flavonoid biosynthesis, and carotenoid biosynthesis, while downregulated DEGs were associated with plant hormone signal transduction, photosynthesis antenna proteins, and transcription factors (Figure S8).

Specifically, the expression levels of key ripening-related genes were significantly altered in the *CR-lncRNA1471* mutant. For example, in ethylene biosynthesis and signal transmission pathways, *SlACS2*, *SlACO3*, and *SlACS4* were significantly upregulated. The ethylene receptors, *SlETR3* (*NR*) and *SlERT4*, were elevated by 3.2-fold and 2.0-fold, respectively, facilitating the effective transmission of ethylene signals to the downstream pathway (Figure 3E). Several classical ripening transcription factors, such as *RIN, CNR, NOR, SlNAC4*, and *SlAP2a,* were markedly upregulated in the *CR-lncRNA1471* mutant (Figure 3E), likely expediting the transition to the BR stage in tomatoes. Additionally, in the carotenoid biosynthesis and metabolism pathway, *SlPSY1* and *SlZISO* were outstandingly upregulated and *SlLCY-e* was downregulated (Figure 3E), which turned the metabolic flux in another branch toward the accumulation of β-carotene in *CR-lncRNA1471* mutants (Figure S5). Several key genes are involved in pectin metabolism, which is crucial for fruit firmness. Genes that negatively regulate pectin biosynthesis, such as *expansins1* (*SlEXP1*), *polygalacturonates* (*SlPG2a*), *tomato β-galactosidase 4* (*SlBG4*), and *pectate lyase* (*SlPL*), were markedly upregulated. In contrast, genes that positively regulate pectin biosynthesis, including *Slβ-subunit*, *xyloglucan hydrolases1* (*SlXTH1*), and *beta-D-xylosidase 2* (*SlXYL*), were downregulated (Figure 3E). Furthermore, *pectinesterase inhibitor-like* (*SlPMEI-like*) displayed a notable 1000-fold upregulation (Figure 3E; Table S1) and negatively regulated pectinesterase *SlPMEU1*, which may decrease pectin accumulation through a structural blockade mechanism (Phan et al., 2007; Wormit & Usadel, 2018). Methylation is a prevalent form of epigenetic regulation along with tomato ripening, the transcriptional expression of genes is activated by demethylation (Liu et al., 2022). Thus, we detected upregulated *SlDML2*-mediated global
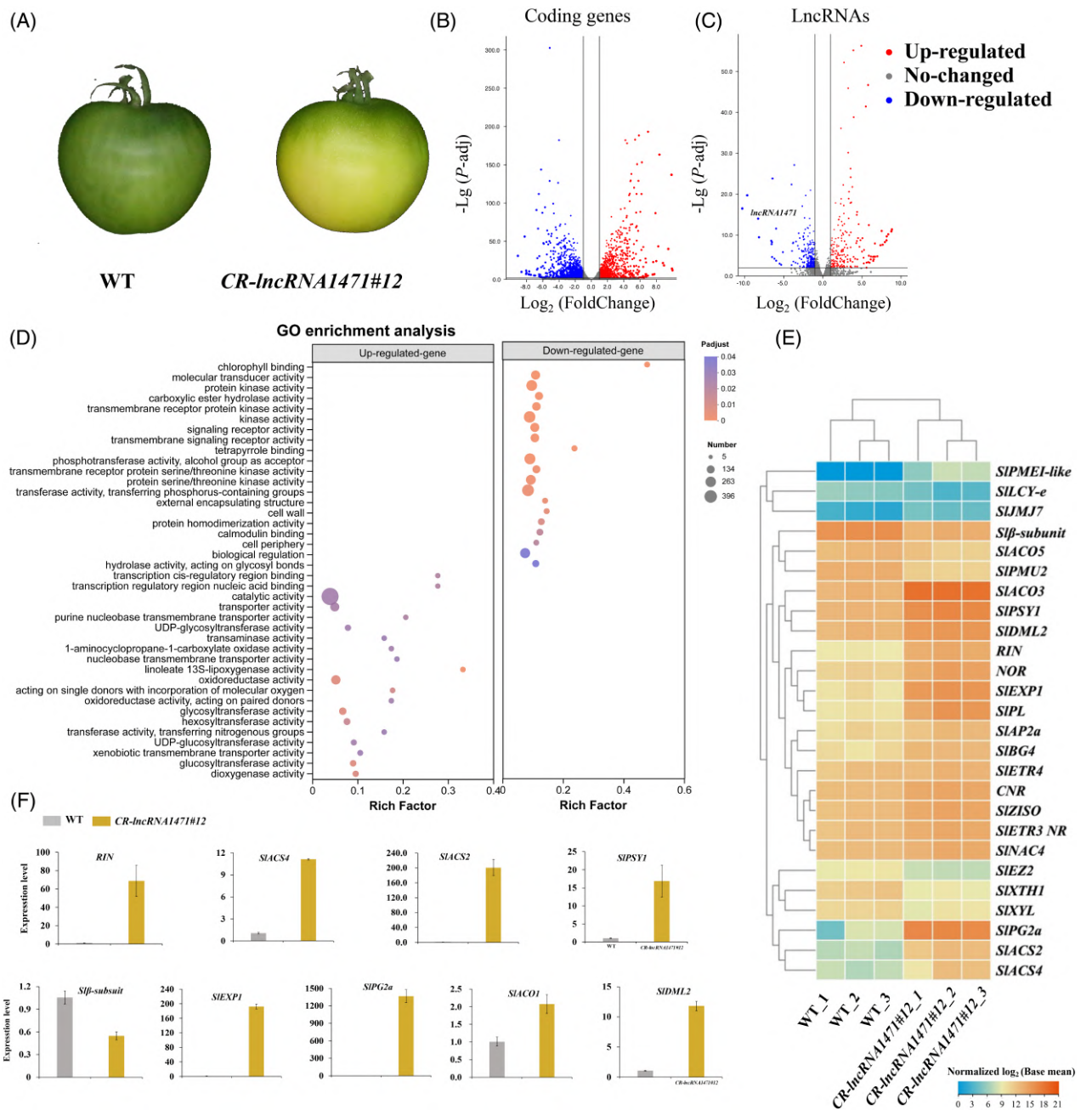
Figure 3. DEGs and DELs were screened on independent homozygous *CR-lncRNA1471#12* mutants and compared to WT in the T1 generation at 40 DPA.
(A) Representative fruit images of WT and *CR-lncRNA1471#12* were used for comparative transcriptome analysis.
(B) Volcano plot visualization of RNA-seq data for coding genes, where each dot represents a gene. The filters were |log2FoldChange|>1 and P_{adj} <0.05.
(C) Volcano plot visualization of RNA-seq data for lncRNAs.
(D) GO enrichment analysis of DEGs in *CR-lncRNA1471#12* compared to WT, the left image illustrates upregulated DEGs, and the right image shows downregulated DEGs.
(E) Heatmap analysis of key ripening-related coding genes in *CR-lncRNA1471#12* compared to WT, and the expression data of DEGs represented as base mean values in the heatmap.
(F) RT-qPCR validation results of representative genes (*SlACS4, SlACS2, SlACO1, RIN, SlEXP1, SlPG2a, SlPSY1, Slβ-subunit,* and *SlDML2*).

DNA hypomethylation, whereas the negative regulators *SlEZ2* (a partner active PRC2 complex) and *SlJMJ7* (an H3K4 demethylase) were downregulated in the *CR-lncRNA1471* mutant, thereby promoting fruit ripening (Figure 3E). Therefore, *lncRNA1471* regulates the key genes involved in ethylene biosynthesis, carotenoid biosynthesis

and metabolism pathways, cell wall metabolism, and methylation processes to participate in tomato ripening. RT-qPCR results for these key genes are shown in Figure 3F.

To determine whether the transcriptional alterations of ripening-related genes were specifically induced by the knockout of *lncRNA1471* rather than by natural ripening itself, a comparative analysis was conducted between the *CR-lncRNA1471#12* mutant and WT from the mature green (MG) stage to the BR stage. The *CR-lncRNA1471#12* mutant (BR/MG) exhibited significantly greater genetic changes than the WT (BR/MG) (Tables S5–S8), such as *SlACS2*, *SlACS4*, *SlACO3*, *SlETR3*, *SlETR4*, *SlPSY1*, *SlEXP1*, *SlPMEI-like*, *RIN*, *CNR*, *SlDML2*, *SlJMJ7*, and others (Figure 4A). This finding suggests that the transcriptional alterations of these key genes were indeed caused by the knockout of *lncRNA1471*. Furthermore, the *CR-lncRNA1471#12* mutant (BR/MG) exhibited 1954 upregulated and 2249 downregulated DEGs (Figure 4B,C). The upregulated DEGs were enriched in protein phosphorylation and regulation of transcription (biological process), DNA binding, and ubiquitin-protein transferase activity (molecular function), as well as in the membrane and nucleus (cellular component) (Figure 4D). Moreover, the downregulated DEGs were involved in the regulation of transcription and metabolic processes (biological processes), transmembrane receptor protein serine/threonine kinase activity, catalytic activity (molecular function), and membrane and nucleus (cellular component) (Figure 4E).

In summary, these findings suggest that *lncRNA1471* primarily engages in ethylene biosynthesis, carotenoid biosynthesis and metabolism pathways, and pectin metabolism by regulating key genes and accelerating the initiation of tomato ripening. According to GO and KEGG analysis, *lncRNA1471* may exert its effects through interactions with transcription factors or protein-binding mechanisms.

LncRNA1471 was identified to bind ASR protein in *vivo* and in *vitro*

Non-coding RNA (ncRNAs), including lncRNAs, rRNA, and tRNA, often assemble with protein cofactors to form extensive ribonucleoprotein complexes, which are crucial for the functional roles of ncRNAs. For example, ncRNAs can regulate gene expression levels by interacting with proteins, and ChIRP-MS is a powerful method for exploring these interactions in *vivo* (Chu, Spitale, & Chang, 2015; Pierouli et al., 2021). To further elucidate the mechanism by which *lncRNA1471* participates in tomato fruit ripening, we conducted ChIRP-MS on the *OE-lncRNA1471* mutants to identify potential *lncRNA1471*-interacting proteins in *vivo*. As detailed in the experimental procedure (Figure 5A), before MS detection, we observed that the enrichment of *lncRNA1471* expression was 30%–80% in the biotin-*lncRNA1471* group using three pairs of independently

designed primers, whereas the biotin-*lacz* group (mock control) did not retrieve *lncRNA1471* (Figure 5B,C). Several potential binding proteins were also present in biotin-*lncRNA1471* samples, as determined by silver staining (Figure S9a). Furthermore, ChIRP-MS identified 17 proteins in the biotin-*lncRNA1471* group, with 7 proteins selected on specific screening criteria (Log$_2$Ratio (biotin-*lncRNA1471*)/(biotin-*lacz*) >3, *P*-value <0.05) (Figure 5D). Interestingly, ASR (Solyc04g071610) was recovered from biotin-*lncRNA1471* groups and is known to function as a transcription factor that influences tomato ripening (Jia et al., 2016). This suggests that *lncRNA1471* may regulate tomato ripening by interacting with the ASR. The roles of the other identified proteins will be explored in future research and are not discussed here.

This study focused on the ASR transcription factor to validate its interaction with *lncRNA1471*. To this end, we conducted a protein pull-down assay in *vitro* using purified His-ASR protein and His-GFP protein (negative control), followed by a PCR assay (Figure S9b,c). We found that *lncRNA1471* was specifically detected in His-ASR-RNA complex samples enriched with His beads, whereas no amplification of *lncRNA1471* was observed in His-GFP-RNA complex samples (negative control) (Figure 5E). Taken together, *lncRNA1471* acts as an important regulator binding to the ASR transcription factor in *vivo* and in *vitro*, thereby influencing the transcription levels of these key ripening-related genes that participate in tomato ripening.

DISCUSSION

This research constitutes a notable advancement in our understanding of the role of lncRNAs in regulating tomato ripening. The knockout of *CR-lncRNA1471* accelerated tomato ripening initiation and induced a range of ripening-related phenotypes. For example, a shorter BR stage, deeper coloration, and increased levels of ethylene, lycopene, and β-carotene, accelerated chlorophyll degradation and fruit firmness reduction (Figure 2). Many key ripening-associated genes, including *SlACS2*, *SlACS4*, *SlPSY1*, *SlZISO*, *SlDML2*, *SlEXP1*, *Slβ-subunit*, *RIN*, and *CNR*, were significantly regulated in the *CR-lncRNA1471* mutant (Figures 3E, 4A). Furthermore, *lncRNA1471* was identified to bind the ASR transcription factor in *vivo* and in *vitro* and might regulate these key genes to participate in tomato fruit ripening. Therefore, *lncRNA1471* functions as an important regulator of tomato-ripening initiation.

The application of the large fragment deletion of *lncRNA1471* serves as a valuable reference for other lncRNAs

Recently, with the advent of advanced sequencing technologies, lncRNAs have become prominent research topics. However, lncRNAs present challenges in exploring their
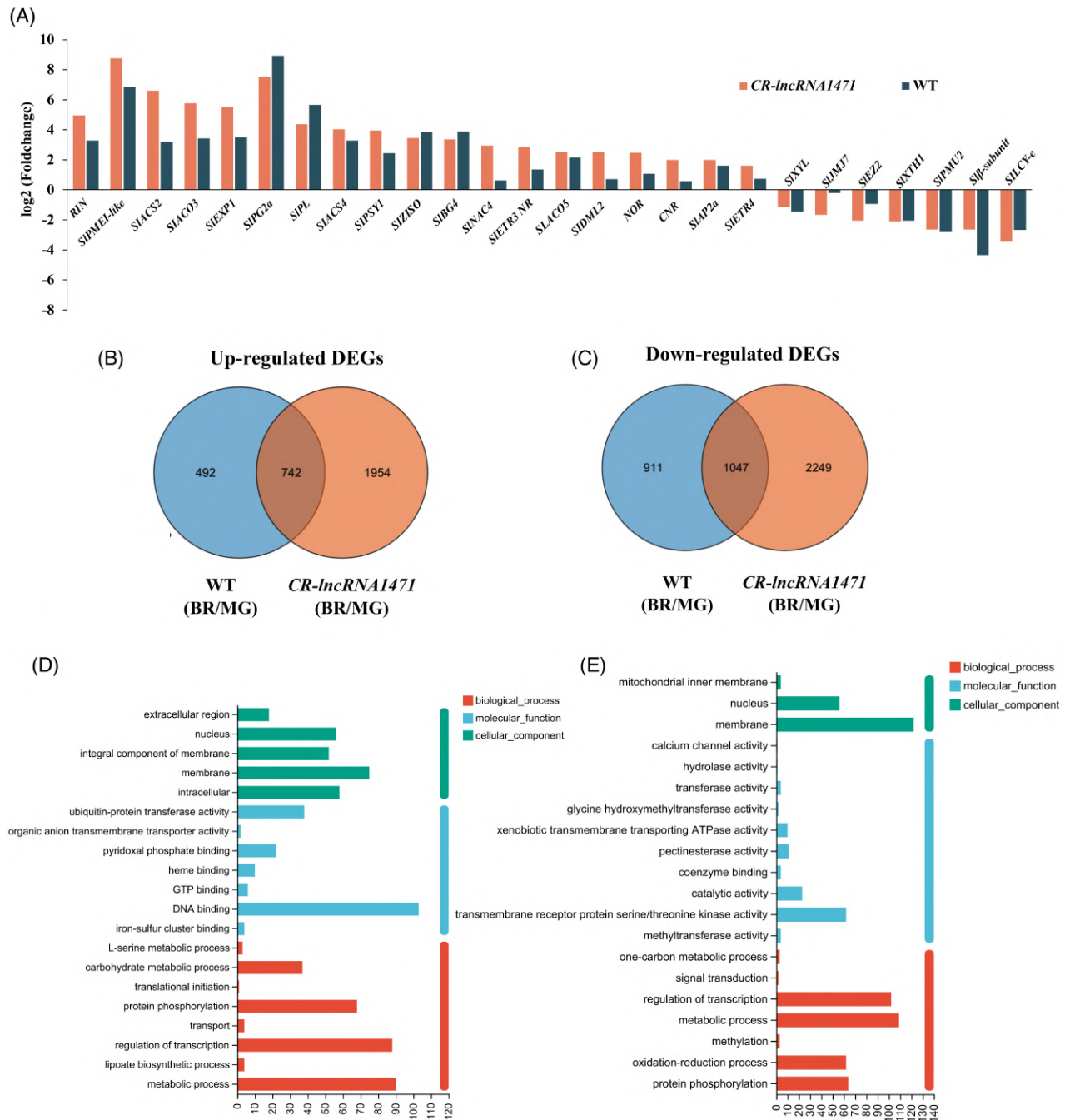
Figure 4. Screening of unique DEGs in *CR-lncRNA1471#12* mutants relative to the normal maturation process from the MG to the BR stage.
(A) The value of $\log_2$ |fold change| for the *CR-lncRNA1471#12* (BR/MG) group compared to the WT (BR/MG) group.
(B, C) Venn diagrams illustrating the upregulated and downregulated DEGs in *CR-lncRNA1471#12* (BR/MG) and WT (BR/MG) groups, respectively. The blue circle represents the WT (BR/MG) group, and the orange circles represent *the CR-lncRNA1471* (BR/MG) group.
(D, E) GO enrichment analysis of specific upregulated and downregulated DEGs in *CR-lncRNA1471#12* mutant, respectively. "BR/MG" means DEGs of the BR stage compared to the MG stage in WT or *lncRNA1471#12* mutant.

biological functions because of low expression levels in tissues and complex secondary structures. Several common transgenic methods have been employed to generate lncRNA knockout or knockdown mutants, including the T-DNA insertion method, RNA interference (RNAi), and

traditional *p*YLCRISPR/Cas9 editing system with a single target (Jin et al., 2023; Li et al., 2018; Rigo et al., 2020). Although these methods have successfully produced mutants of target lncRNAs, they do not completely delete the target lncRNA sequence, thereby potentially omitting
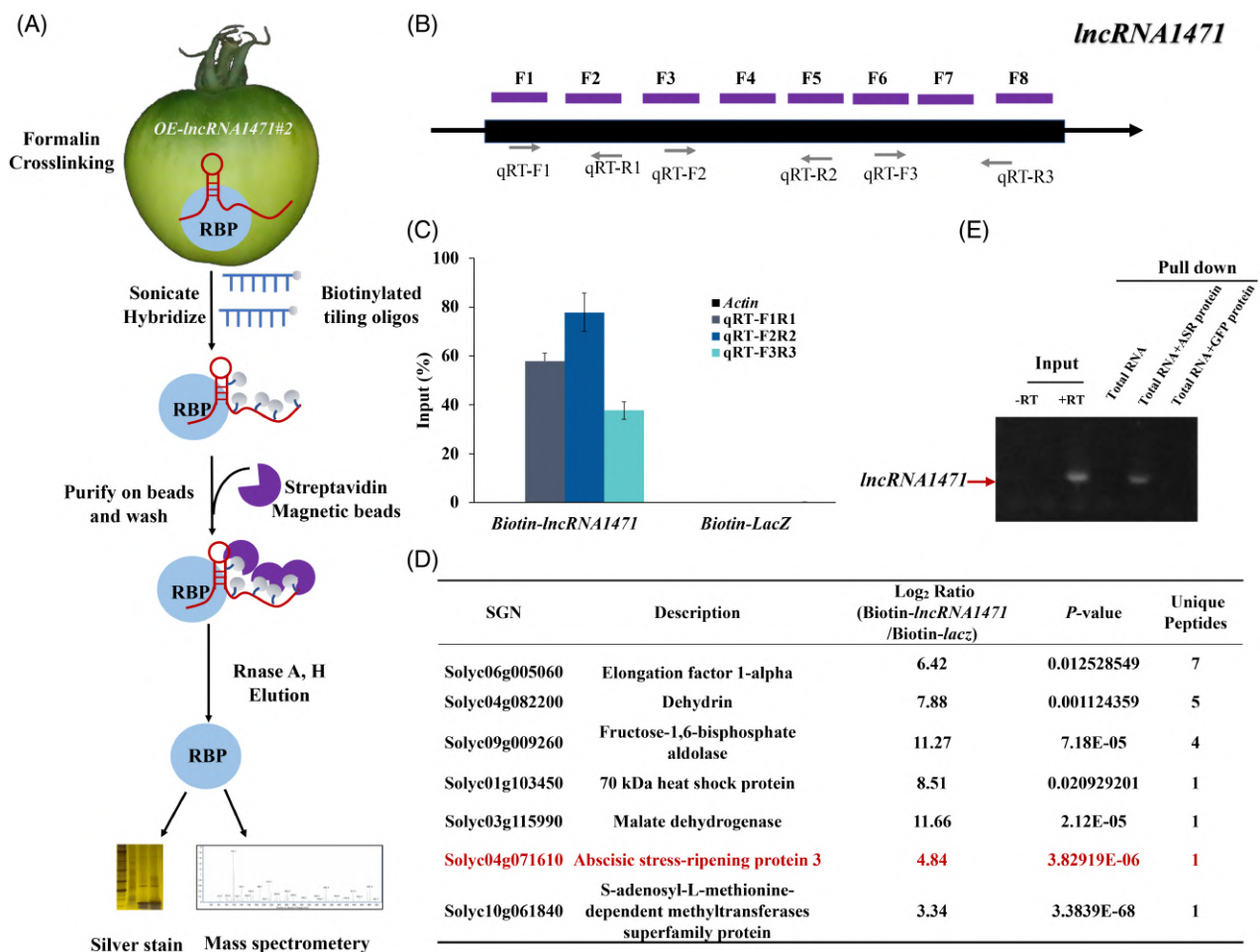
Figure 5. Identification of potential binding protein of *lncRNA1471*.
(A) Depiction of the experimental procedures for ChIRP-MS.
(B) Antisense RNA probes and three pairs of indecent primers were designed within the exon region of *lncRNA1471*. The purple frame represents eight probes targeting the *lncRNA1471* sequence, labeled F1–F8.
(C) The enrichment rate of *lncRNA1471* in the biotin-*lncRNA1471* groups and biotin-lacz groups (mock control) with *actin* used as the normalization gene.
(D) Information on potential *lncRNA1471* binding proteins, including SGN number, description, log$_2$Ratio, *P*-value, and unique peptides. The log$_2$Ratio was calculated using normalized MS peak intensities of biotin-*lncRNA1471* groups compared to biotin-lacz groups.
(E) Testing the binding of *lncRNA1471* to its target protein was conducted using His-ASR and His-GFP (negative control). Binding interactions with *lncRNA1471* transcripts were evaluated using PCR.

crucial biological information. For example, traditional CRISPR/Cas9 technology hardly directly affects the secondary structure of lncRNAs, which is critical for governing their functional roles (Zhu et al., 2023). In this study, an advanced CRISPR-Cas9 system with double-reverse pairs of sgRNAs strategy enabled the large fragment deletion of *lncRNA1471* (Figure 1F). This represents a successful application of lncRNA editing to achieve large fragment deletions and obtain stable genetic modifications. Although the editing efficiency of the advanced editing technology for the *CR-lncRNA1471* mutant was 11.8% in the T0 generation, this approach yielded more accurate and abundant information on the lncRNAs. Moreover, with the emergence of polysome profiling or sequencing of the ribosome, some lncRNAs were proven to encode functional

micropeptides (Ruiz-Orera et al., 2014). Thus, the encoded micropeptides of *lncRNA1471* need more evidence to validate and will be discussed in future research. Therefore, the advanced CRISPR-Cas9 system makes it easy to obtain large fragment deletions and provides more precise biological function information for target lncRNAs. Therefore, this study offers a reference for successful lncRNA editing and has significant implications for lncRNAs.

LncRNA1471 acts as a negative regulator for the initiation of tomato ripening

Fruit ripening is crucial to seed dispersal and fruit quality (Alba et al., 2005). Several positive and negative regulators influence the initiation and progression of tomato ripening. On the one hand, positive regulatory

factors influence the tomato-ripening procession, for example, hydrogen-sulfide-repressed methionine synthase (*SlMS*) (Geng et al., 2022), the RNA-editing factor *SlORRM4* (Yang, Liu, et al., 2020), *lncRNA2155* and *lncRNA1459* (Li et al., 2018; Yu et al., 2019), as well as O-glycosylation enzymes *SPINDLY* (*SPY*) (Xu et al., 2023). Additionally, several positive regulators mediate the initiation of tomato ripening, including various NAC transcription factors, such as *NOR-like1*, *SlNAC4*, and *SlNAM1* (Gao et al., 2018; Gao et al., 2021; Zhu et al., 2014), as well as the brassinosteroid signaling component *SlBZR1* (Meng et al., 2023). In contrast, recent studies have identified that the transcriptional repressor *MYB70* and H3K4 demethylase *SlJMJ7* negatively regulate the tomato-ripening procession (Cao et al., 2020; Ding et al., 2022). Furthermore, knockdown of the downstream genes of the AP2/ERF-domain family *SlDREB3* and abscisic acid co-receptor type 2C phosphatase (PP2C3) accelerates the initiation of tomato ripening by mediating ABA metabolism and sensitivity, respectively (Gupta et al., 2022; Liang et al., 2021). In this study, knockout of *lncRNA1471* promoted tomato-ripening initiation, thus, *lncRNA1471* was identified as another negative regulator that may mediate ripening-related genes by interacting with the ASR transcript factor. Additionally, previous reports have observed that key transcription factors influence fruit ripening and metabolite accumulation, particularly carotenoids and sugars (Jia et al., 2024). Furthermore, DEGs in the *lncRNA1471* mutant may affect metabolite profiles by enriching carotenoid synthesis and polyphenols, contributing to tomato ripening. Importantly, a comparison analysis is presented in this research to exclude the possibility of normal development itself causing tomato ripening. Therefore, negative regulators of tomato ripening are less well documented, and the discovery of *lncRNA1471* adds novel evidence to the negative regulation network of tomato ripening.

ChIRP-MS is an effective method to identify the interacting protein of lncRNAs

The ChIRP-MS method can identify potential interacting proteins of most ncRNAs in *vivo*. Through self-building ChIRP-MS, the researcher first discovered that Xist, an essential lncRNA involved in X-chromosome inactivation (XCI), interacts with 81 human proteins (Chu, Zhang, et al., 2015). Furthermore, lncRNA *MISSEN* has been reported to regulate tubulin function by hijacking the HeFP protein using the ChIRP-MS method (Zhou et al., 2021). In this study, ChIRP-MS analysis revealed that *lncRNA1471* may interact with seven proteins to regulate tomato ripening. Among these, the ASR protein has emerged as a promising candidate because the *OE-ASR* mutants previously accelerated fruit ripening and softening, whereas the RNAi plant line delayed fruit ripening (Jia et al., 2016). In addition, *asr* mutants usually affect the transcription levels of ripening-related genes, such as *ASC2* and *ACO1*

(Dominguez et al., 2021). Moreover, *lncRNA1471* did not affect the transcriptional level of *ASR*, suggesting that *lncRNA1471* may regulate ASR protein levels via post-transcriptional mechanisms. Furthermore, we confirmed that *lncRNA1471* binds to the purified His-ASR protein in *vitro* (Figure 5E; Figure S9b,c). Therefore, these results indicate that *lncRNA1471* may regulate key genes by interacting with the ASR protein to participate in tomato ripening. Regarding other proteins, the EF1α (Solyc06g00060) is mainly involved in the translation of eukaryotic proteins by mediating the interaction between aminyl-tRNA and ribosomes and is implicated in drought stress and crop yield in rice (Dever & Green, 2012; Gu et al., 2023). However, the relationship between fruit ripening and *EF1α* expression has not yet been reported. EF1α may influence the final translation outcome or contribute to the dynamic synthesis of ripening-related proteins. This hypothesis requires further validation using proteomic analysis or polysome profiling. The dehydrin protein (Soly04g082200) has been reported to participate in cold stress in tomatoes and drought tolerance in tea plant progenies (Gupta et al., 2012; Weiss & Egea-Cortines, 2009). The upstream signaling pathway of dehydrin, which includes ABA, mitogen-activated protein kinase (MAPK), and Ca^{2+}, regulates the transcription of dehydrin (Zolotarov & Strömvik, 2015). It is conceivable that *lncRNA1471* regulates the upstream signaling pathway and consequently influences the accumulation of dehydrin protein. A potential binding protein, the s-adenosyl-L-methionine-dependent methyltransferase superfamily protein (solyc10g061840), primarily regulates plant growth, plant pigment levels, antioxidant activity, and signal transducers (Cheng et al., 2003; Hui et al., 2015; Roldan et al., 2014; Zubieta et al., 2003). The proteins that participate in tomato ripening require further investigation and are not discussed herein.

In this study, although we verified the interaction between *lncRNA1471* and ASR protein, which usually showed a *trans*-mode, the *cis*-acting of *lncRNA1471* should not be ignored. Recent studies have identified three potential *cis*-acting mechanisms of lncRNAs. (I) lncRNAs recruit regulatory factors to the locus of the gene through its transcript. (II) The transcription and splicing of lncRNAs may contribute to neighboring genes. (III) DNA regulatory elements within the lncRNA promoter or gene body affect regulatory mechanisms (Kopp & Mendell, 2018). Therefore, we also focused on the neighboring genes within the 100 kb upstream and downstream regions of *lncRNA1471*, and 27 candidate cis-regulated target genes were predicted. Among these, seven genes exhibited significant differences ($|\log_2 FoldChange|>2$). We found that *lncRNA1471* most likely regulates the expression of solyc03g111970, assigned to cytochrome P450 (CYP), located 1.5 kb upstream, by influencing its promoter. Moreover, CYP

detoxifies xenobiotics involved in NADPH- and O_2-dependent hydroxylation processes and serves as a growth and developmental signal (Chakraborty et al., 2023; Jun et al., 2015). Therefore, *lncRNA1471* regulates CYP to participate in tomato ripening, but this requires extensive and direct evidence. Consequently, although *lncRNA1471* may be involved *in cis*-acting mechanisms, we believe that *trans*-action was dominant in this study.

In summary, our findings suggested that *lncRNA1471* acts as a negative regulator and promotes the initiation of tomato ripening. This effect is attributed to the comprehensive coordination of multiple regulatory aspects mediated by *lncRNA1471*, including the ethylene-related pathway, carotenoid biosynthesis and metabolism pathway, cell wall metabolism, and ripening-related demethylation processes. Additionally, *lncRNA1471* was identified to interact with the ASR transcription factor and regulated the key genes involved in tomato ripening. The discovery of *lncRNA1471* enhances our understanding of the regulatory landscape of fruit ripening and offers valuable insights into the mechanisms underlying fruit ripening from the perspective of lncRNAs.

EXPERIMENTAL PROCEDURES

Plant materials and growth conditions

Tomato (*Solanum lycopersicum cv.* Ailsa Craig) was cultivated in glasshouses under a 16-h light/8-h dark cycle at 20–25°C. Tissues from both transgenic and WT plants were harvested and immediately frozen in liquid nitrogen, followed by storage at −80°C for subsequent analysis.

Cloning the full-length lncRNA

Total RNA was extracted from tomato leaves using an E.Z.N.A. Plant RNA Kit (Omega, Georgia, USA, cat. no. R6827). For 3′cDNA synthesis, a FirstChoice RLM-RACE Kit (Invitrogen, Waltham, MA, USA; cat. no. AM1700) was employed along with oligo primers and specific primers to get 3′polyA tail sequence. For 5′cDNA synthesis, aliquots of 1 μg RNA were reverse transcribed using the HiScript II 1st Strand cDNA Synthesis Kit (Vazyme Biotech, Beijing, China; cat. no. R212) using specific primers. The full-length lncRNA sequence was cloned from the cDNA. The amplified fragments were determined by Sanger sequencing. Relevant primers used are listed in Table S9.

Expression patterns of *lncRNA1471* in tomato tissues

We analyzed the expression pattern of *lncRNA1471* across various tissues of tomatoes, including the roots, stems, leaves, flowers, and fruits. Total RNA was extracted from these tissues and cDNA was synthesized. RT-qPCR was performed using Taq-Pro Universal SYBR qPCR Master Mix (Vazyme Biotech, Beijing, China; cat. no. Q712) on a CFX96 Touch Real-Time PCR Detection System (Bio-Rad, https://www.bio-rad.com/). Relative mRNA expression levels were calculated using the $2^{-\Delta\Delta Ct}$ method with *actin* as an internal reference gene for normalization. Each experiment included three biological and three technical replicates. The qRT-PCR primers that were used are listed in Table S9.

Nuclear cytoplasmic fractionation

Nuclear cytoplasmic fractionation was performed as previously described (Wang et al., 2011). Tomato fruits were harvested at 49 DPA for fractionation. RNA was extracted from the nucleus and cytoplasm using TRIzol reagent. *U6* and *actin* served as the internal reference genes for the nuclear and cytoplasmic fractions, respectively. Experiments were conducted using three biological replicates. The specific primers used to calculate enrichment rates are listed in Table S9.

The related transgenic plants were obtained

Double-reverse pairs of sgRNAs were designed to obtain *lncRNA1471* knockout mutants with large fragment deletions by using the pYLCRISPR-Cas9 plasmid. As described in our previous study (Zhu et al., 2023), we designed two reverse pairs of sgRNAs targeting the upstream and downstream regions of *lncRNA1471*. sgRNAs were designed and optimized using an online tool (http://skl.scau.edu.cn/targetdesign/) that is recommended for CRISPR-Cas9 target selection. Several screening criteria have been applied for the design of sgRNAs. For instance, the GC% of sgRNAs was maintained between 40% and 70% and sequences with more than four consecutive T nucleotides (>4) were avoided. sgRNA expression cassettes were generated using overlapping PCR to ensure precise construction. The target sequence was ligated into the corresponding promoter and sgRNA regions during the first PCR round. The *BsaI* restriction site was introduced in the second PCR round. Subsequently, the four sgRNA expression cassettes were assembled into the *pYCRISPR-Cas9-Ubi-H* binary plasmid using the Golden Gate ligation method (Ma et al., 2015). In this advanced strategy, a pair of primers (For and Rev, shown in Figure 1e) was designed at the ends of *lncRNA1471* with a genomic interval of 3.7 kb to detect large fragment deletion. If the strategy had been successful, a 483-bp fragment would have been amplified. Additionally, *lncRNA1471* overexpression transgenic plants were generated using the *p*CAMBIA1300 plasmid. The *lncRNA1471*-related plasmid was introduced into the AC tomato cultivar via *Agrobacterium tumefaciens*-mediated transformation. The primers used in this assay are listed in Table S9.

The phenotype measurement and analysis

To measure fruit BR days, we recorded the flowering date and calculated the total number of days required from flowering to fruit reaching the BR stage, which was expressed as the DPA exceeding 100 samples. To assess ethylene production and respiratory rate, the fruit was stored at 25°C for 4 h following harvest and then sealed in a container at 25°C for an additional 2 h. Gas (1 mL) was drawn using a syringe for measurement by gas chromatography (GC-14, Shimadzu, https://www.shimadzu.com/). The values were calculated using the following formula: ethylene production (nL/gh) = $C_{ppm} \times (V_{mL}-m_g)/(m_g \times T_h)$, and the respiratory rate (mg × CO_2/gh) = $A_{ppm} \times (V_{mL}-m_g) \times 44/22\,400 \times (m_g \times T_h)$, where C_{ppm} and A_{ppm} denote the quantities of ethylene production and CO_2 release, respectively. Additionally, V_{mL}, m_g, and T_h represent the volume of the container, fruit weight, and sealing time, respectively. A handheld hardness tester (GY-5B, Quzhou Aipu Measuring Instrument Co., Ltd., China) was used to measure the fruit hardness. A handheld precision colorimeter (Shenzhen Threenh Technology Co., Ltd, China, NR110) was used to record the a* value (a* value represents the degree of red color of fruits) and measured four points along the equatorial position of tomato fruits. For the 1-MCP treatment, 3.5% 1-MCP was applied to different tomato fruit lines at the BR stage for 16 h. The treated fruits

were then stored under a 16 h light/8 h dark at 20–25°C and photo-graphed. The chlorophyll content was determined using a method previously described (Powell et al., 2012). The lycopene and β-carotene contents were also determined using a previously published method (Zhang et al., 2024).

Transcriptome data analysis

Three biological replicates of WT and *CR-lncRNA#12* mutant at 40 DPA, as well as WT at the BR stage (44 DPA) and *CR-lncRNA#12* at the MG stage (36 DPA), were sequenced using a strand-specific method (2 × 150 bp). The quality of the clean data was obtained using the FastpQC software. All clean data were aligned with the tomato reference genome (SGN release v.SL2.5). In addition, lncRNAs were mapped against ripening-related lncRNA libraries constructed in our laboratory. Both coding genes and lncRNAs were processed using Hisat2.0. The read counts and fold changes of these genes were obtained using Feature-Counts and DESeq2.R, respectively. The basemean count exhibited the gene expression value, and the fold change was determined to be basemean$_{lncRNA1471}$/basemean$_{WT}$, basemean$_{lncRNA1471-BR}$/basemean$_{lncRNA1471-MG}$, and basemean$_{WT-BR}$/basemean$_{WT-MG}$. Transcriptome data were analyzed to identify DEGs or DELs between the *CR-lncRNA1471* mutant and WT at 40 PDA by applying a screening criterion (*P*-adj <0.05, |log$_2$FoldChange|>1).

PCA and KEGG enrichment analysis

Correlation analysis of the three biological replicates within each group was performed using PCA with SIMCA (version 14.1). DEGs were subjected to the KEGG pathway analysis using TBtool (version 1.0) (Chen et al., 2023). Upregulated and downregulated DEGs were analyzed separately.

ChIRP-MS analysis

The ChIRP-MS method was performed according to the method described (Chu & Chang, 2018), and the experimental procedure is illustrated in Figure 5A. Eight antisense probes were designed at 100 bp intervals along the full-length sequence of *lncRNA1471*, while four antisense probes were designed against the *Lacz* sequence (mock control) (Figure 5B). All probes with biotin-tri-ethylene glycol (TEG) attached to the 3′end were synthesized by Sanger Biotech Co. Ltd. (Beijing, China). *OE-lncRNA1471#2* fruits at the BR stage were collected and crosslinked with glutaralde-hyde to preserve RNA–protein interactions and then quenched using 0.125 M glycine for 5 min. The cross-linked samples were ground in liquid nitrogen and stored at −80°C. Powder samples (1.0 g) were diluted with twice-volume lysis buffer (50 mM Tris–HCl pH 7.0, 10 mM EDTA, 1% SDS, 1 mM PMSF, Proteinase Inhibitor 50X (0.01v), RNase Inhibitor 200X (0.01v)) and then centrifuged at 16000*g* at 4°C for 15 min. The samples were subsequently soni-cated using a non-contact ultrasonic instrument (30 sec ON, 5 sec OFF, 100% W, 30 min). A 1/100 volume sample was reserved as input, while the target *lncRNA1471* was hybridized with probes and isolated using Dynabeads™ MyOne™ Streptavidin C1 beads (Invitrogen, Waltham, MA, USA; cat. no. 65001), and 1 μL of the probe (100 μM) was added to 1 mL of lysis buffer. The separated products were washed with a high-salt washing buffer (2 × SSC, 0.5% SDS, 1 mM DTT, and 1 mM PMSF). To determine the enrich-ment rate of *lncRNA1471* in biotin-*lncRNA1471* and biotin-*lacz* samples, RNA was extracted from the separated bead-bound products using an RNA elution buffer (100 mM NaCl, 10 mM Tris–HCl pH 7.0, 1 mM EDTA, 0.5% SDS, and 5% v/v proteinase K fresh). The remaining bead samples were treated with elution buffer (20 mM Tris–HCl pH 7.5, 2 mM CaCl$_2$) to obtain

lncRNA1471-binding proteins and then subjected to hydrolysis using sequencing-grade trypsin to obtain peptide segments, which were subsequently analyzed by mass spectrometry (Orbi-trap Fusion Lumos Tribrid, Thermo Fisher, USA). Additionally, the protein bands were detected using the ProteoSilver™ Plus Silver Stain Kit (Sigma, SL Louis, USA, SLCD4365) before MS detection. Experiments were conducted using three biological replicates. The probe sequences used are listed in Table S10.

Expression and Purification of ASR and GFP protein

For the ASR protein, the cDNA sequence was amplified by PCR from an RNA template generated from the tomato fruit. The green fluorescent protein (GFP) protein sequence was obtained from the *p*CAMBIA-35 s-GFP vector. The two target cDNA fragments were cloned into a *p*QE-80 L vector containing an N-terminal His-tag fusion using a one-step cloning kit (Vazyme Biotech, Beijing, China; cat. no. C112-02). The two recombinant vectors were intro-duced into *E. coli* expression strain BL21(DE3) cells to facilitate the expression. And then induced by adding 0.8 nM IPTG at 37°C for 4 h. Subsequently, the bacterial cell precipitate was suspended in His-binding buffer (20 mM Tris–HCl pH 7.4, 500 mM NaCl, 10 mM imidazole) supplemented with 20 mg/mL lysozyme, 10 mg/mL protease inhibitor, and 100 mM PMSF. The cell suspension was incubated on ice for 30 min, followed by sonication at 50% maxi-mum power for 4 sec on/6 sec off for 20 min on ice. The superna-tant was applied to a Solarbio® His-Tag Resin column affinity (Ni2+) (Solarbio Science & Technology Co., Ltd, Beijing, China; cat. no. P2010) and incubated on ice for 2 h, and washed sequen-tially with His binding buffer, 20 mM washing buffer (50 mM Tris–HCl (pH = 7.4), 150 mM NaCl, 20 mM imidazole), 80 mM washing buffer (200 mM Tris–HCl (pH = 7.4), 600 mM NaCl, 80 mM imidaz-ole), 500 mM washing buffer (1.25 M Tris–HCl (pH = 7.4), 3.75 mM NaCl, 500 mM imidazole). The washed sample (500 μL) was con-centrated using an ultrafiltration tube by centrifugation at 6000 rpm for 4 h at 4°C to get ASR and GFP purification protein. Purified proteins were visualized using the Coomassie Brilliant Blue Fast Staining solution (Solarbio Science & Technology Co., Ltd, Beijing, China, cat. no. P1300). For His-tag protein immuno-blot analysis, the primary antibody targeting His-tag (Abmart, Shanghai, China; cat. no. M30111M) was used at a 1:5000 dilution, whereas secondary goat anti-mouse IgG (MBL, Nagoya, Japan; cat. no. 330) at 1:10000 dilution. Then, the blots were visualized using an enhanced chemiluminescence kit (Absin, Shanghai, China; cat. no. abs920), and imaging was performed using a Tanon-5200 imager (Tanon Science & Technology, Shanghai, China).

Protein pull-down assay

Protein pull-down assays were performed as previously described (Tian et al., 2019). Total RNA was extracted from *OE-lncRNA1471* fruits at the BR stage, heated to 95°C for 2 min, and slowly cooled to room temperature. Folded total RNA was stored using Dynabead™ His-Tag (Thermo Fisher Scientific, Waltham, MA, USA; cat. no. 10103D) in pull-down buffer (6.5 mM sodium phos-phate pH 7.4, 140 mM NaCl, 0.02% Tween-20, and 40-U/mL RNase inhibitor). His-ASR or His-GFP proteins (2 μg) were bound to Dynabeads in a binding buffer (100 mM sodium phosphate pH 7.4, 600 mM NaCl, 1 mM PMSF, and 0.02% Tween-20) and then incubated at 4°C for 30 min. The ASR-RNA and GFP-RNA com-plexes were subsequently eluted with His-elution buffer (50 mM sodium phosphate pH 8.0, 300 mM NaCl, 0.01% Tween-20, and 300 mM imidazole) at 4°C for 10 min. The enriched RNAs were recovered using the TRIzol extraction method and subsequently analyzed using RT-PCR. The primers used are listed in Table S9.

Statistical analysis

AUTHOR CONTRIBUTIONS

LZ designed and performed experiments and wrote the manuscript. LZ and TL analyzed the RNA-seq data. HZ, LM, and GZ provided funding support. GQ, BZ, DF, and YL provided the technical support for this study. ARS assisted with language modifications.

ACKNOWLEDGEMENTS

CONFLICT OF INTEREST STATEMENT

All authors have no conflicts of competing interests to declare for this manuscript submission.

DATA AVAILABILITY STATEMENT

All data are available in the main text or supplementary material.

SUPPORTING INFORMATION

Additional Supporting Information may be found in the online version of this article.

Figure S1. Full-length sequence of *lncRNA1471*, with yellow letters denoting the 5′cDNA sequence and 3′RACE fragment sequence.

Figure S2. Electrophoretic bands of the amplified genes. (a) Electrophoretic bands corresponding to the residual fragment following the deletion of full-length *lncRNA1471* in various *CR-lncRNA1471* homozygous mutants of the T1 generation. (b) Electrophoretic bands associated with hygromycin in different *CR-lncRNA1471* homozygous mutants of the T1 generation.

Figure S3. The expression levels of *lncRNA1471* in various *OE-lncRNA1471* mutant plant lines #1 through #19 of the T0 generation, and the expression level of *lncRNA1471* in the WT, were used as the reference standard, and was normalized to the *actin* expression level.

Figure S4. 1-MCP treated representative independent homozygous mutants, including *CR-lncRNA1471#12, OE-lncRNA1471#2*, and WT, at the BR stage. The air treatment served as a control. "0 h" represents the time point immediately before 1-MCP treatment, and "0 day" refers to the 0th day of treatment initiation.

Figure S5. β-arotene content was measured in representative independent homozygous mutants, including *CR-lncRNA1471#12, OE-lncRNA1471#2*, and WT at 46 DPA, 49 DPA, and 52 DPA. Samples marked with different lowercase letters indicate statistically significant differences ($P < 0.05$). Error bars indicate the mean ± SD of three biological replicates.

Figure S6. Chlorophyll (CHl a, CHl b, and CHls a + b) content was measured in representative independent homozygous mutants, including *CR-lncRNA1471#12, OE-lncRNA1471#2*, and WT at 40 DPA. Samples marked with lowercase letters represent statistically significant differences ($P < 0.05$). Error bars indicate the mean ± SD of three biological replicates.

Figure S7. Correlation analysis was conducted on three biological replicates of representative independent homozygous mutants, including *CR-lncRNA1471#12* and WT at 40 DPA in the T1 generation using PCA analysis. The samples labeled *as CR-1471_7_2, CR-1471_9_1*, and *CR-1471_9_2* corresponded to *CR-lncRNA1471#12_1, CR-lncRNA1471#12_2*, and *CR-lncRNA1471#12_3*, respectively.

Figure S8. KEGG pathway enrichment analysis of DEGs in the *CR-lncRNA1471#12* mutant at 40 DPA in the T1 generation. (a) Enrichment analysis of the upregulated DEGs. (b) Enrichment analysis of the downregulated DEGs.

Figure S9. Silver staining was performed to identify potential *lncRNA1471*-interacting proteins, and affinity purification using Ni2+ was conducted to isolate tomato His-ASR and His-GFP proteins. (a) Silver staining results for potential *lncRNA1471*-interacting proteins, with the biotin-*lacz* group serving as a mock control. (b, c) Purified tomato His-ASR protein and His-GFP protein were separated by SDS-PAGE and visualized by staining with Coomassie Brilliant Blue. Lane 1, 20 μL aliquots of bacterial culture without 0.8 mM IPTG. Lane 2, 20 μL aliquots of bacterial culture with 0.8 mM IPTG. Lane 3, 0.5 μg of purified protein. (d, e) The identification of His-ASR and His-GFP was performed using western blot analysis. Lane 1, 20 μL aliquots of bacterial culture without 0.8 mM IPTG. Lane 2, 20 μL aliquots of bacterial culture with 0.8 mM IPTG. Lane 3, 1xloading buffer. Lane 4, 0.5 μg of purified protein.

Table S1. Up-regulated DEGs in *CR-lncRNA1471#12* mutant compared to WT in 40 DPA.

Table S2. Down-regulated DEGs in *CR-lncRNA1471#12* mutant compared to WT in 40 DPA.

Table S3. Up-regulated DELs in *CR-lncRNA1471#12* mutants compared to WT in 40 DPA.

Table S4. Down-regulated DELs in *CR-lncRNA1471#12* mutants compared to WT in 40 DPA.

Table S5. Upregulated DEGs at the BR stage compared to the MG stage in WT.

Table S6. Downregulated DEGs at the BR stage compared to those at the MG stage in WT.

Table S7. Up-regulated DEGs at the BR stage compared to the MG stage in *CR-lncRNA1471#12* mutant.

Table S8. Down-regulated DEGs at the BR stage compared to the MG stage in *CR-lncRNA1471#12* mutant.

Table S9. The complete sequence of all primers utilized in this research.

Table S10. The complete sequence of all probes used in the ChIRP-MS analysis in this research.

REFERENCES

Alba, R., Payton, P., Fei, Z.J., McQuinn, R., Debbie, P., Martin, G.B. *et al.* (2005) Transcriptome and selected metabolite analyses reveal multiple points of ethylene control during tomato fruit development. *Plant Cell*, **17**, 2954–2965.

Ariel, F., Jegu, T., Latrasse, D., Romero-Barrios, N., Christ, A., Benhamed, M. *et al.* (2014) Noncoding transcription by alternative RNA polymerases dynamically regulates an auxin-driven chromatin loop. *Molecular Cell*, **55**, 383–396.

Barry, C.S., McQuinn, R.P., Thompson, A.J., Seymour, G.B., Grierson, D. & Giovannoni, J.J. (2005) Ethylene insensitivity conferred by the Green-ripe and Never-ripe 2 ripening mutants of tomato. *Plant Physiology*, **138**, 267–275.

Borsani, O., **Zhu, J.H.**, **Verslues, P.E.**, **Sunkar, R.** & **Zhu, J.K.** (2005) Endogenous siRNAs derived from a pair of natural cis-antisense transcripts regulate salt tolerance in Arabidopsis. *Cell*, **123**, 1279–1291.

Cao, H., **Chen, J.**, **Yue, M.**, **Xu, C.**, **Jian, W.**, **Liu, Y.** *et al.* (2020) Tomato transcriptional repressor MYB70 directly regulates ethylene-dependent fruit ripening. *The Plant Journal*, **104**, 1568–1581.

Chakraborty, P., **Biswas, A.**, **Dey, S.**, **Bhattacharjee, T.** & **Chakrabarty, S.** (2023) Cytochrome P450 Gene Families: Role in Plant Secondary Metabolites Production and Plant Defense. *Journal of Xenobiotics*, **13**, 402–423.

Chen, C.J., **Wu, Y.**, **Li, J.W.**, **Wang, X.**, **Zeng, Z.H.**, **Xu, J.** *et al.* (2023) TBtools-II: A "one for all, all for one" bioinformatics platform for biological big-data mining. *Molecular Plant*, **16**, 1733–1742.

Chen, Y.T., **Cheng, C.Z.**, **Feng, X.**, **Lai, R.L.**, **Gao, M.X.**, **Chen, W.G.** *et al.* (2021) Integrated analysis of lncRNA and mRNA transcriptomes reveals the potential regulatory role of lncRNA in kiwifruit ripening and softening. *Scientific Report UK*, **11**(1), 1671.

Cheng, Z.G., **Sattler, S.**, **Maeda, H.**, **Sakuragi, Y.**, **Bryant, D.A.** & **DellaPenna, D.** (2003) Highly divergent methyltransferases catalyze a conserved reaction in tocopherol and plastoquinone synthesis in cyanobacteria and photosynthetic eukaryotes. *Plant Cell*, **15**, 2343–2356.

Chu, C. & **Chang, H.Y.** (2018) ChIRP-MS: RNA-Directed Proteomic Discovery. *Methods in Molecular Biology*, **1861**, 37–45.

Chu, C., **Spitale, R.C.** & **Chang, H.Y.** (2015) Technologies to probe functions and mechanisms of long noncoding RNAs. *Nature Structural & Molecular Biology*, **22**(1), 29–35.

Chu, C., **Zhang, Q.F.C.**, **da Rocha, S.T.**, **Flynn, R.A.**, **Bharadwaj, M.**, **Calabrese, J.M.** *et al.* (2015) Systematic Discovery of Xist RNA Binding Proteins. *Cell*, **161**, 404–416.

Deng, H., **Chen, Y.**, **Liu, Z.Y.**, **Liu, Z.Q.**, **Shu, P.**, **Wang, R.C.** *et al.* (2022) SlERF.F12 modulates the transition to ripening in tomato fruit by recruiting the co-repressor TOPLESS and histone deacetylases to repress key ripening genes. *Plant Cell*, **34**, 1250–1272.

Dever, T.E. & **Green, R.** (2012) The Elongation, Termination, and Recycling Phases of Translation in Eukaryotes. *Cold Spring Harbor Perspectives in Biology*, **4**(7), a013706.

Dey, S.S., **Sharma, P.K.**, **Munshi, A.D.**, **Jaiswal, S.**, **Behera, T.K.**, **Kumari, K.** *et al.* (2022) Genome wide identification of lncRNAs and circRNAs having regulatory role in fruit shelf life in health crop cucumber (Cucumis sativus L.). *Frontiers in Plant Science*, **13**, 884476.

Ding, X.C., **Liu, X.C.**, **Jiang, G.X.**, **Li, Z.W.**, **Song, Y.B.**, **Zhang, D.D.** *et al.* (2022) SlJMJ7 orchestrates tomato fruit ripening via crosstalk between H3K4me3 and DML2-mediated DNA demethylation. *New Phytologist*, **233**, 1202–1219.

Dominguez, P.G., **Conti, G.**, **Duffy, T.**, **Insani, M.**, **Alseekh, S.**, **Asurmendi, S.** *et al.* (2021) Multiomics analyses reveal the roles of the ASR1 transcription factor in tomato fruits. *Journal of Experimental Botany*, **72**, 6490–6509.

Fraser, P.D., **Truesdale, M.R.**, **Bird, C.R.**, **Schuch, W.** & **Bramley, P.M.** (1994) Carotenoid Biosynthesis during Tomato Fruit-Development. *Plant Physiology*, **105**, 405–413.

Gao, Y., **Fan, Z.Q.**, **Zhang, Q.**, **Li, H.L.**, **Liu, G.S.**, **Jing, Y.** *et al.* (2021) A tomato NAC transcription factor, SlNAM1, positively regulates ethylene biosynthesis and the onset of tomato fruit ripening. *The Plant Journal*, **108**, 1317–1331.

Gao, Y., **Wei, W.**, **Zhao, X.D.**, **Tan, X.L.**, **Fan, Z.Q.**, **Zhang, Y.P.** *et al.* (2018) A NAC transcription factor, NOR-like1, is a new positive regulator of tomato fruit ripening. *Hortic Res-England*, **5**, 75.

Geng, Z.K., **Ma, L.**, **Rong, Y.L.**, **Li, W.J.**, **Yao, G.F.**, **Zhang, H.** *et al.* (2022) A hydrogen-sulfide-repressed methionine synthase slMS1 acts as a positive regulator for fruit ripening in tomato. *International Journal of Molecular Sciences*, **23**(20), 12239.

Giovannoni, J.J. (2004) Genetic regulation of fruit development and ripening. *Plant Cell*, **16**, S170–S180.

Gu, Q., **Kang, J.F.**, **Gao, S.**, **Zhao, Y.R.**, **Yi, H.** & **Zha, X.J.** (2023) Eukaryotic translation elongation factor OsEF1A positively regulates drought tolerance and yield in rice. *Plants-Basel*, **12**(14), 2593.

Guo, S.S., **Zheng, Y.Y.**, **Meng, D.M.**, **Zhao, X.Y.**, **Sang, Z.Z.**, **Tan, J.J.** *et al.* (2022) DNA and coding/non-coding RNA methylation analysis provide insights into tomato fruit ripening. *The Plant Journal*, **112**, 399–413.

Gupta, A., **Upadhyay, R.K.**, **Prabhakar, R.**, **Tiwari, N.**, **Garg, R.**, **Sane, V.A.** *et al.* (2022) a negative regulator of ABA responses, controls seed germination, fruit size and the onset of ripening in tomato. *Plant Science*, **319**, 111249.

Gupta, S., **Bharalee, R.**, **Bhorali, P.**, **Bandyopadhyay, T.**, **Gohain, B.**, **Agarwal, N.** *et al.* (2012) Identification of drought tolerant progenies in tea by gene expression analysis. *Functional & Integrative Genomics*, **12**, 543–563.

Hu, G., **Huang, B.**, **Wang, K.**, **Frasse, P.**, **Maza, E.**, **Djari, A.** *et al.* (2021) Histone posttranslational modifications rather than DNA methylation underlie gene reprogramming in pollination-dependent and pollination-independent fruit set in tomato. *The New Phytologist*, **229**, 902–919.

Hui, D., **Wu, J.**, **Ji, K.-X.**, **Zeng, Q.-Y.**, **Bhuiya, M.-W.** *et al.* (2015) Methylation mediated by an anthocyanin, O-methyltransferase, is involved in purple flower coloration in Paeonia. *Journal of Experimental Botany*, **66**(21), 6563–6577.

Jia, H., **Xu, Y.**, **Deng, Y.**, **Xie, Y.**, **Gao, Z.**, **Lang, Z.** *et al.* (2024) Key transcription factors regulate fruit ripening and metabolite accumulation in tomato. *Plant Physiology*, **195**, 2256–2273.

Jia, H.F., **Jiu, S.T.**, **Zhang, C.**, **Wang, C.**, **Tariq, P.**, **Liu, Z.J.** *et al.* (2016) Abscisic acid and sucrose regulate tomato and strawberry fruit ripening through the abscisic acid-stress-ripening transcription factor. *Plant Biotechnology Journal*, **14**, 2045–2065.

Jin, Y., **Ivanov, M.**, **Dittrich, A.N.**, **Nelson, A.D.L.** & **Marquardt, S.** (2023) LncRNA FLAIL affects alternative splicing and represses flowering in Arabidopsis. *The EMBO Journal*, **42**(11), e110921.

Jun, X.U., **Xin-Yu, W.** & **Wang-Zhen, G.** (2015) The cytochrome P450 superfamily: Key players in plant development and defense. *Journal of Integrative Agriculture*, **14**, 1673–1686.

Kopp, F. & **Mendell, J.T.** (2018) Functional Classification and Experimental Dissection of Long Noncoding RNAs. *Cell*, **172**, 393–407.

Li, R., **Fu, D.Q.**, **Zhu, B.Z.**, **Luo, Y.B.** & **Zhu, H.L.** (2018) CRISPR/Cas9-mediated mutagenesis of lncRNA1459 alters tomato fruit ripening. *The Plant Journal*, **94**, 513–524.

Li, S.G., **Zhang, J.Y.**, **Zhang, L.Q.**, **Fang, X.P.**, **Luo, J.**, **An, H.S.** *et al.* (2022) Genome-wide identification and comprehensive analysis reveal potential roles of long non-coding RNAs in fruit development of southern highbush blueberry (*Vaccinium corymbosum* L.). *Frontiers in Plant Science*, **13**(13), 1078085.

Liang, B., **Sun, Y.F.**, **Wang, J.**, **Zheng, Y.**, **Zhang, W.B.**, **Xu, Y.D.** *et al.* (2021) Tomato protein phosphatase 2C influences the onset of fruit ripening and fruit glossiness. *Journal of Experimental Botany*, **72**, 2403–2418.

Liu, Z., **Wu, X.**, **Liu, H.**, **Zhang, M.** & **Liao, W.** (2022) DNA methylation in tomato fruit ripening. *Physiologia Plantarum*, **174**, e13627.

Ma, X.L., **Zhang, Q.Y.**, **Zhu, Q.L.**, **Liu, W.**, **Chen, Y.**, **Qiu, R.** *et al.* (2015) A Robust CRISPR/Cas9 System for Convenient, High-Efficiency Multiplex Genome Editing in Monocot and Dicot Plants. *Molecular Plant*, **8**, 1274–1284.

Manning, K., **Tör, M.**, **Poole, M.**, **Hong, Y.**, **Thompson, A.J.**, **King, G.J.** *et al.* (2006) A naturally occurring epigenetic mutation in a gene encoding an SBP-box transcription factor inhibits tomato fruit ripening. *Nature Genetics*, **38**, 948–952.

Meng, F.L., **Liu, H.R.**, **Hu, S.S.**, **Jia, C.G.**, **Zhang, M.**, **Li, S.W.** *et al.* (2023) The brassinosteroid signaling component SlBZR1 promotes tomato fruit ripening and carotenoid accumulation. *Journal of Integrative Plant Biology*, **65**, 1794–1813.

Nakatsuka, A., **Murachi, S.**, **Okunishi, H.**, **Shiomi, S.**, **Nakano, R.**, **Kubo, Y.** *et al.* (1998) Differential expression and internal feedback regulation of 1-aminocyclopropane-1-carboxylate synthase, 1-aminocyclopropane-1-carboxylate oxidase, and ethylene receptor genes in tomato fruit during development and ripening. *Plant Physiology*, **118**, 1295–1305.

Phan, T.D., **Bo, W.**, **West, G.**, **Lycett, G.W.** & **Tucker, G.A.** (2007) Silencing of the Major Salt-Dependent Isoform of Pectinesterase in Tomato Alters Fruit Softening. *Plant Physiology*, **144**, 1960–1967.

Pierouli, K., **Goulielmos, G.N.**, **Eliopoulos, E.** & **Vlachakis, D.** (2021) Genome regulation by long non-coding RNAs. *EMBnet Journal*, **26**(Suppl A), e962.

Powell, A.L.T., **Nguyen, C.V.**, **Hill, T.**, **Cheng, K.L.**, **Figueroa-Balderas, R.**, **Aktas, H.** *et al.* (2012) Uniform ripening encodes a Golden 2-like transcription factor regulating tomato fruit chloroplast development. *Science*, **336**, 1711–1715.

Qin, G.Z., **Wang, Y.Y.**, **Cao, B.H.**, **Wang, W.H.** & **Tian, S.P.** (2012) Unraveling the regulatory network of the MADS box transcription factor RIN in fruit ripening. *The Plant Journal*, **70**, 243–255.

Rigo, R., Bazin, J., Romero-Barrios, N., Moison, M., Lucero, L., Christ, A. et al. (2020) The Arabidopsis lncRNA *ASCO* modulates the transcriptome through interaction with splicing factors. *EMBO Reports*, **21**(5), e48977.

Roldan, M.V.G., Outchkourov, N., van Houwelingen, A., Lammers, M., de la Fuente, I.R., Ziklo, N. et al. (2014) An O-methyltransferase modifies accumulation of methylated anthocyanins in seedlings of tomato. *The Plant Journal*, **80**, 695–708.

Ruiz-Orera, J., Messeguer, X., Subirana, J.A. & Alba, M.M. (2014) Long non-coding RNAs as a source of new peptides. *eLife*, **16**(3), e03523.

Tang, Y.J., Qu, Z.P., Lei, J.J., He, R.Q., Adelson, D.L., Zhu, Y.L. et al. (2021) The long noncoding RNA *FRILAIR* regulates strawberry fruit ripening by functioning as a noncanonical target mimic. *PLoS Genetics*, **17**(3), e1009461.

Thomson, D.W. & Dinger, M.E. (2016) Endogenous microRNA sponges: evidence and controversy. *Nature Reviews, Genetics*, **17**, 272–283.

Tian, Y.Y., Bai, S.L.G., Dang, Z.H., Hao, J.F., Zhang, J. & Hasi, A. (2019) Genome-wide identification and characterization of long non-coding RNAs involved in fruit ripening and the climacteric in Cucumis melo. *BMC Plant Biology*, **19**(1), 369.

Vrebalov, J., Ruezinsky, D., Padmanabhan, V., White, R., Medrano, D., Drake, R. et al. (2002) A MADS-box gene necessary for fruit ripening at the tomato ripening-inhibitor (*rin*) locus. *Science*, **296**, 343–346.

Wang, W., Ye, R., Xin, Y., Fang, X., Li, C., Shi, H. et al. (2011) An importin beta protein negatively regulates MicroRNA activity in *Arabidopsis*. *Plant Cell*, **23**, 3565–3576.

Weiss, J. & Egea-Cortines, M. (2009) Transcriptomic analysis of cold response in tomato fruits identifies dehydrin as a marker of cold stress. *Journal of Applied Genetics*, **50**, 311–319.

Wierzbicki, A.T., Blevins, T. & Swiezewski, S. (2021) Long Noncoding RNAs in Plants. *Annual Review of Plant Biology*, **72**, 245–271.

Wilusz, J.E., Sunwoo, H. & Spector, D.L. (2009) Long noncoding RNAs: functional surprises from the RNA world. *Genes & Development*, **23**, 1494–1504.

Wormit, A. & Usadel, B. (2018) The Multifaceted Role of Pectin Methylesterase Inhibitors (PMEIs). *International Journal of Molecular Sciences*, **19** (10), 2878.

Wu, M.B., Liu, K.D., Li, H.H., Li, Y., Zhu, Y.Q., Su, D. et al. (2024) Gibberellins involved in fruit ripening and softening by mediating multiple hormonal signals in tomato. *Hortic Res-England*, **11**(2), uhad275.

Xu, J., Liu, S.D., Cai, L.C., Wang, L.Y., Dong, Y.F., Qi, Z.Y. et al. (2023) SPIN-DLY interacts with EIN2 to facilitate ethylene signalling-mediated fruit ripening in tomato. *Plant Biotechnology Journal*, **21**, 219–231.

Yang, M.M., Zhu, S.B., Jiao, B.Z., Duan, M., Meng, Q.W., Ma, N.N. et al. (2020) SISGRL, a tomato SGR-like protein, promotes chlorophyll degradation downstream of the ABA signaling pathway. *Plant Physiology and Biochemistry*, **157**, 316–327.

Yang, Y.F., Liu, X.Y., Wang, K.R., Li, J.Y., Zhu, G.N., Ren, S. et al. (2020) Molecular and functional diversity of organelle RNA editing mediated by RNA recognition motif-containing protein *ORRM4* in tomato. *New Phytologist*, **228**, 570–585.

Yang, Y.F., Zhu, G.N., Li, R., Yan, S.J., Fu, D.Q., Zhu, B.Z. et al. (2017) The RNA editing factor *SIORRM4* is required for normal fruit ripening in tomato. *Plant Physiology*, **175**, 1690–1702.

Yang, Y.W., Liu, T.L., Shen, D.Y., Wang, J.Y., Ling, X.T., Hu, Z.Z. et al. (2019) Tomato yellow leaf curl virus intergenic siRNAs target a host long non-coding RNA to modulate disease symptoms. *PLoS Pathogens*, **15**(1), e1007534.

Yu, T.T., Tzeng, D.T.W., Li, R., Chen, J.Y., Zhong, S.L., Fu, D.Q. et al. (2019) Genome-wide identification of long non-coding RNA targets of the tomato MADS box transcription factor RIN and function analysis. *Annals of Botany London*, **123**, 469–482.

Yu, Y.T., Liufu, Y.X., Ren, Y., Zhang, J., Li, M.Y., Tian, S.W. et al. (2023) Comprehensive profiling of alternative splicing and alternative polyadenylation during fruit ripening in watermelon (*Citrullus lanatus*). *International Journal of Molecular Sciences*, **24**(20), 15333.

Zhang, P., Wang, Y., Zhu, G. & Zhu, H. (2024) Developing carotenoids-enhanced tomato fruit with multi-transgene stacking strategies. *Plant Physiology and Biochemistry*, **210**, 108575.

Zhong, S.L., Fei, Z.J., Chen, Y.R., Zheng, Y., Huang, M.Y., Vrebalov, J. et al. (2013) Single-base resolution methylomes of tomato fruit development reveal epigenome modifications associated with ripening. *Nature Biotechnology*, **31**, 154–159.

Zhou, Y.F., Zhang, Y.C., Sun, Y.M., Yu, Y., Lei, M.Q., Yang, Y.W. et al. (2021) The parent-of-origin lncRNA *MISSEN* regulates rice endosperm development. *Nature Communications*, **12**(1), 6525.

Zhu, B.Z., Yang, Y.F., Li, R., Fu, D.Q., Wen, L.W., Luo, Y.B. et al. (2015) RNA sequencing and functional analysis implicate the regulatory role of long non-coding RNAs in tomato fruit ripening. *Journal of Experimental Botany*, **66**, 4483–4495.

Zhu, G., Li, R., Zhang, L., Ma, L., Li, J., Chen, J. et al. (2024) RNA-protein interactions reveals the pivotal role of *lncRNA1840* in tomato fruit maturation. *The Plant Journal*, **120**(2), 526–539.

Zhu, G.N., Zhang, L.L., Ma, L.Q., Liu, Q., Wang, K.J., Li, J.Y. et al. (2023) Efficient large fragment deletion in plants: double pairs of sgRNAs are better than dual sgRNAs. *Hortic Res-England*, **10**(10), uhad168.

Zhu, M.K., Chen, G.P., Zhou, S., Tu, Y., Wang, Y., Dong, T.T. et al. (2014) A new tomato NAC (NAM/ATAF1/2/CUC2) transcription factor, SINAC4, functions as a positive regulator of fruit ripening and carotenoid accumulation. *Plant & Cell Physiology*, **55**, 119–135.

Zolotarov, Y. & Strömvik, M. (2015) Regulatory motif discovery identifies significant motifs in promoters of five classes of plant dehydrin genes. *PLoS One*, **10**(6), e0129016.

Zubieta, C., Ross, J.R., Koscheski, P., Yang, Y., Pichersky, E. & Noel, J.P. (2003) Structural basis for substrate recognition in the salicylic acid carboxyl methyltransferase family. *Plant Cell*, **15**, 1704–1716.